Acta Crystallographica Section D
Biological Crystallography
ISSN 0907-4449

Direct cryocooling of naked crystals: are cryoprotection agents always necessary?

Erika Pellegrini,[a,b] Dario Piano[a]‡ and Matthew W. Bowler[a]*

[a]Structural Biology Group, European Synchrotron Radiation Facility, 6 Rue Jules Horowitz, F-38043 Grenoble, France, and [b]Department of Molecular Biology and Biotechnology, University of Sheffield, Sheffield S10 2TN, England

‡ Current address: Unit of Botany, Department of Life and Environmental Sciences, Viale Sant'Ignazio da Laconi 13, 09123 Cagliari, Italy.

Correspondence e-mail: bowler@esrf.fr

Received 6 May 2011
Accepted 2 August 2011

Over the last 20 years cryocrystallography has revolutionized the field of macromolecular crystallography, greatly reducing radiation damage and allowing the collection of complete data sets at synchrotron sources. However, in order to cool crystals to 100 K cryoprotective agents must usually be added to prevent the formation of crystalline ice, which disrupts the macromolecular crystal lattice and often results in a degradation of diffraction quality. This process can involve the extensive testing of solution compositions and soaking protocols to find suitable conditions that maintain diffraction quality. In this study, it is demonstrated that when some crystals of macromolecules are mounted in the complete absence of surrounding liquid no crystalline ice is formed and the diffraction resolution, merging R factors and mosaic spread values are comparable to those of crystals cryocooled in the presence of a cryoprotectant. This potentially removes one of the most onerous manual steps in the structure-solution pipeline and could alleviate some of the foreseen difficulties in the automation of crystal mounting.

1. Introduction

Macromolecular crystallographic data collection at synchrotron sources is almost invariably performed at 100 K in order to reduce the effects that ionizing radiation has on crystals. In order to cool crystals of macromolecules to these temperatures, it is usually necessary to add a cryoprotective agent to the mother liquor surrounding the crystal in order to prevent the formation of ice crystals that can damage the crystal lattice. Cryoprotection is successful when sufficient cryoprotectant is added such that the solution surrounding the crystal forms an amorphous glass, no diffraction is observed from crystalline ice and the diffraction properties of the crystals are maintained (Garman & Schneider, 1997; Parkin & Hope, 1998; Weik & Colletier, 2010; Garman, 1999; Teng, 1990; Rodgers, 1994; Pflugrath, 2004; Juers & Matthews, 2004*b*). Finding an optimal cryoprotection solution is often a matter of randomly screening a large number of conditions, although progress has been made in the rational design of cryoprotection protocols (Alcorn & Juers, 2010; Juers & Matthews, 2004*a*; Garman & Mitchell, 1996; Berejnov *et al.*, 2006; Chinte *et al.*, 2005).

It has been observed that some crystals do not require the addition of a cryoprotective agent after controlled dehydration (Bowler *et al.*, 2006; Kiefersauer *et al.*, 2000; Russi *et al.*, 2011; Sanchez-Weatherby *et al.*, 2009; Zerrad *et al.*, 2011). In such experiments, all surrounding mother liquor is removed from a crystal before it is subjected to a dehydration protocol. Once a beneficial phase change has been induced, the crystal is usually directly cryocooled for subsequent data collection; no cryoprotective agent is required and the diffraction resolution and mosaic spread of the uncooled crystals are retained. This behaviour was attributed to the complete absence of mother liquor surrounding the crystal and was assumed to be peculiar to the dehydration process itself. Previous work has shown that the partial removal of mother liquor reduces the required concentration of cryoprotectant agent (Kwong & Liu, 1999; Thorne *et al.*, 2003; Hope, 1988) and it has been suggested that complete removal could allow direct cryocooling (Warkentin *et al.*, 2006). A liquid-free mounting method has also been described (Kitago *et al.*, 2005), although in this

Table 1
Data-processing statistics for crystals of trypsin, β-PGM, RhoA, hPGK and hPGK–L-ADP cryocooled without surrounding liquid and using standard cryoprotectant solutions.

Values in parentheses are for the highest resolution bin.

Protein	Trypsin	Trypsin	β-PGM–G6P–MgF_3^-	β-PGM–G6P–MgF_3^-	RhoA	RhoA	hPGK	hPGK	hPGK–L-ADP
Precipitant	1.9 *M* $(NH_4)_2SO_4$	1.9 *M* $(NH_4)_2SO_4$	24% PEG 4000	24% PEG 4000	24% PEG 3350	24% PEG 3350	28% PEG 2000 MME	28% PEG 2000 MME	28% PEG 2000 MME
Cryoprotectant	None	20% glycerol	None	20% PEG 400	None	20% EG	None	35% PEG 2000 MME	None
Space group	$P2_12_12_1$	$P2_12_12_1$	$P2_12_12_1$	$P2_12_12_1$	$P2_12_12_1$	$P2_12_12_1$	$P2_12_12_1$	$P2_12_12_1$	$P2_12_12_1$
Beamline	ID14-2	ID14-2	ID14-1	ID14-1	ID14-1	ID14-2	ID23-1	ID23-1	ID23-2
Wavelength (Å)	0.933	0.933	0.932	0.932	0.932	0.933	0.979	0.979	0.873
Unit-cell parameters (Å)									
a	54.4	54.5	37.2	37.7	31.8	32.1	38.8	39.3,	38.4
b	58.2	58.2	54.2	54.1	66.0	65.7	90.6	92.0	103.9
c	66.5	67.0	104.6	103.9	83.6	83.8	108.6	108.7	203.1
Resolution range (Å)	20–1.39 (1.46–1.39)	20–1.37 (1.44–1.37)	20–1.33 (1.40–1.33)	20–1.38 (1.46–1.38)	20–1.60 (1.69–1.60)	20–1.80 (1.90–1.80)	20–1.80 (1.90–1.80)	20–1.82 (1.92–1.82)	20–2.90 (3.06–2.90)
No. of unique reflections	37604	33263	46171	54734	21758	17096	35450	36023	17028
Multiplicity	4.6 (4.2)	3.2 (1.2)	3.4 (3.0)	2.7 (2.6)	2.6 (1.7)	4.2 (4.3)	4.1 (3.9)	4.7 (4.8)	3.0 (3.1)
Completeness (%)	87.8 (97.4)	72.8 (14.2†)	94.0 (76.6)	98.3 (98.7)	91.4 (66.9)	99.9 (100.0)	97.7 (95.0)	99.0 (97.8)	90.7 (99.1)
R_{merge}‡	0.06 (0.35)	0.06 (0.39)	0.05 (0.45)	0.03 (0.10)	0.03 (0.12)	0.04 (0.73)	0.05 (0.52)	0.06 (0.56)	0.13 (0.51)
$\langle I/\sigma(I)\rangle$	14.5 (3.2)	15.6 (2.4)	18.7 (2.4)	21.3 (7.9)	23.0 (5.2)	19.7 (2.1)	14.1 (2.5)	14.5 (4.8)	7.7 (2.3)
Wilson *B* factor (Å^2)	9.4	7.6	10.6	7.7	16.9	29.8	27.4	29.5	60
Average mosaic spread (°)	0.49	0.54	0.30	0.39	0.53	0.57	0.70	0.57	0.80
Solvent content (%)	46	46	47	47	47	47	44	44	45
Solvent-channel diameter (largest dimension) (Å)	20	20	19	19	19	19	20	20	25

† The completeness for the cryoprotected trypsin crystal is low at high resolution as these data were only collected at the corners of the detector. ‡ $R_{merge} = \sum_{hkl}\sum_i |I_i(hkl) - \langle I(hkl)\rangle|/\sum_{hkl}\sum_i I_i(hkl)$, where $\langle I(hkl)\rangle$ is the mean weighted intensity after rejection of outliers.

case a penetrative cryoprotectant was added in advance. Here, we show that several crystal systems can be successfully cryocooled without the addition of any penetrative cryoprotectant by simply removing the mother liquor surrounding the crystal. This method of cryoprotection removes the need to screen for cryoprotective agents and avoids mechanical damage to crystals by reducing the number of handling steps. As no liquid remains surrounding the crystal, background X-ray scattering and absorption are reduced and crystals are easier to visualize. Crystal harvesting remains the last entirely manual step in the gene-to-structure pipeline, but some progress has been made in automating the process (Berger *et al.*, 2010; Kitago *et al.*, 2010; Viola *et al.*, 2007). If generally applicable, the method outlined here obviates the requirement to search for suitable cryoprotection solutions and the need for automated soaking protocols; this should help to simplify the process of automated crystal harvesting.

2. Experimental procedures

2.1. Crystal preparation

Bovine pancreatic trypsin (Sigma–Aldrich) was resuspended at a concentration of 40 mg ml^{-1} in a buffer consisting of 10 m*M* benzamidine and 3 m*M* $CaCl_2$. Equal amounts of this solution were then mixed with precipitant solution (1.9 *M* ammonium sulfate and 0.1 *M* Tris pH 8.5) in hanging drops (2 + 2 µl). These crystals are usually cryoprotected using mother liquor with 20% glycerol added. Crystals of the closed conformation of β-phosphoglucomutase (β-PGM) from *Lactobacillus lactis* were obtained from 26–30% PEG 4000, 200 m*M* sodium acetate and 100 m*M* Tris pH 7.5 and are normally cryoprotected by the addition of 20% PEG 400 to the mother liquor (Baxter *et al.*, 2010). Human phosphoglycerate kinase (hPGK) in complex with AlF_4^-, 3PG and either D-ADP or L-ADP was crystallized in 28% PEG 2000 MME and 0.1 *M* Bis-Tris pH 6.5. These crystals are usually cryoprotected by increasing the concentration of PEG 2000 MME to 35% (Cliff *et al.*, 2010; Lallemand *et al.*, 2011). Recombinant human RhoA was expressed as a GST fusion in *Escherichia coli* BL21 (DE3) cells and purified by affinity chromatography followed by removal of the GST tag by thrombin cleavage and size-exclusion chromatography. RhoA–GDP–AlF_4^- crystals were obtained at 293 K by the sitting-drop method from solutions consisting of 10 mg ml^{-1} RhoA, 50 m*M* MES pH 5.5, 150 m*M* NaCl, 5 m*M* $MgCl_2$, 1 m*M* DTT, 1 m*M* $AlCl_3$, 10 m*M* NaF, 10 m*M* GDP equilibrated against 24%(*w*/*v*) PEG 3350 and 0.3 *M* NaCl. These crystals are normally cryoprotected by the addition of 25% ethylene glycol to the mother liquor. The purification and crystallization of DR2577 from *Deinococcus radiodurans* (DR) will be described elsewhere.

2.2. Cryocooling naked crystals

All crystals were mounted using MicroMesh loops (MiTeGen, Ithaca, New York, USA) with a 10 µm mesh size, except for crystals of the membrane protein DR2577, which were mounted using a 25 µm mesh-size loop. Large crystals were scooped out with the meshes, whereas microcrystals were swept out. In both cases all mother liquor was removed by touching the reverse of the mesh to laboratory tissue paper (Kimtech KimWipes, Kimberly Clark, Irving, Texas, USA) prior to flash-cooling in a cold gaseous nitrogen stream or plunging directly into liquid nitrogen. Complete removal of the mother liquor reduces the sample size to that of the crystal, thereby reducing the thermal diffusion time and increasing the rate of cooling. Estimates of the cooling rates of this technique, based on previous observations (Teng & Moffat, 1998), are 110 K s^{-1} for gaseous nitrogen and 183 K s^{-1} for liquid nitrogen.

2.3. Diffraction data collection

The successful cryocooling of crystals was assessed by collecting diffraction images. All data were collected on the ESRF Structural Biology Beamlines, Grenoble, France. Data-collection strategies were calculated using *EDNA*/*BEST* (Incardona *et al.*, 2009; Bourenkov & Popov, 2010) executed through the *MXCuBE* beamline GUI

(Gabadinho *et al.*, 2010). Data sets from crystals of bovine pancreatic trypsin were collected using an ADSC Q4R CCD detector on beamline ID14-2 (λ = 0.933 Å). For *β*-PGM and RhoA data sets were collected using an ADSC Q210 CCD detector on beamline ID14-1 (λ = 0.932 Å) and an ADSC Q4R CCD detector on beamline ID14-2 (λ = 0.933 Å). For hPGK data were collected using an ADSC Q315 CCD detector on beamline ID23-1 (λ = 0.979 Å). For microneedle crystals of L-ADP-bound hPGK data were collected using a MAR Mosaic 225 detector on the microfocus beamline ID23-2 using a helical data-collection strategy (Flot *et al.*, 2010) over an area defined by diffraction cartography (Bowler *et al.*, 2010). Diffraction data from crystals of DR2577 were collected using a PILATUS 6M detector on beamline ID29 (λ = 0.976 Å) with a beam size of 10 µm (see Table 1).

3. Results and discussion

To test the general use of this naked crystal (no cryoprotectant) cooling method, we applied the protocol to several different systems. The crystals used in this study varied from those with a largest dimension of 600 µm that diffracted to high resolution down to 10 µm crystals with a diffraction limit of around 15 Å. In all cases, the complete removal of surrounding liquid resulted in successful cryocooling of the crystals (Figs. 1 and 2). For five of these cases we collected data sets that were of excellent quality and of comparable quality to those collected from crystals that had had a cryoprotectant added (Table 1). For the microneedles of hPGK crystallized with L-ADP it was additionally advantageous to avoid a cryosolution owing to the paucity of the L-enantiomer of the nucleotide; here, L-ADP was only added to the protein solution, reducing the amount required. For the crystals of the DR membrane protein DR2577 this method of cryocooling was essential as crystals of this size were lost in cryosolutions and the correct matching of detergent concentrations between crystallization solutions and cryosolutions can be problematic. We directly cryocooled crystals on a dry mesh, enabling easy visualization of the crystals, and diffraction was observed to ∼15 Å resolution, indicating that the crystals were protein and that the conditions were worth pursuing.

How does the removal of surrounding liquid cryoprotect macromolecular crystals? Cryoprotection using oils usually requires the complete removal of mother liquor before cryocooling, as does the slow cooling of protein crystals (Warkentin & Thorne, 2009; Hope, 1988), as the solvent in the channels of macromolecular crystals acts differently to that surrounding the crystal. The complete removal of mother liquor changes the composition of a typical sample from mostly solvent containing a crystal to a crystal containing around 50% solvent. Detailed studies of the glass transition of the solvent within crystals have shown that the size of the channels, rather than the total solvent content, influences the crystallization of the water within them (Weik *et al.*, 2001). The hydration shell that surrounds proteins can extend to a maximum of 8 Å (Jiang & Brünger, 1994; Chen *et al.*, 2008) and owing to the influence of the protein surface these water molecules will behave differently from those in the bulk solvent. This implies that water molecules in solvent channels of up to 16 Å in diameter will be affected by the protein surface and prevent the formation of crystalline ice, but this may probably be larger owing to the nonzero critical nucleation radius of cubic ice (20 Å). In the cases presented here the protein itself is probably acting as the cryoprotectant by inhibiting the formation of crystalline ice within the solvent channels. The maximum allowable solvent-channel diameter for this cryocooling technique can be measured using crystals of bovine mitochondrial F_1-ATPase. Controlled dehydration of these crystals reduces the unit-cell volume by 20% and the solvent content from 64 to 56% and a number of stable intermediates exist in the dehydration pathway (Bowler *et al.*, 2006; Sanchez-Weatherby *et al.*, 2009). After the dehydration process, crystals can be directly cryocooled; however, when attempting to cryocool the intermediate states it became apparent that this was not possible, as diffraction from these crystals was not observed after cryocooling. As only the final dehydrated state can be cryocooled without the addition of a cryoprotectant, we can define the threshold maximum diameter of the solvent channels that can support this method of cryocooling. The largest solvent channel in the undehydrated crystals has dimensions of 75 × 51 Å. In the state closest to the final dehydrated state that is still not capable of direct cryocooling, the dimensions have been

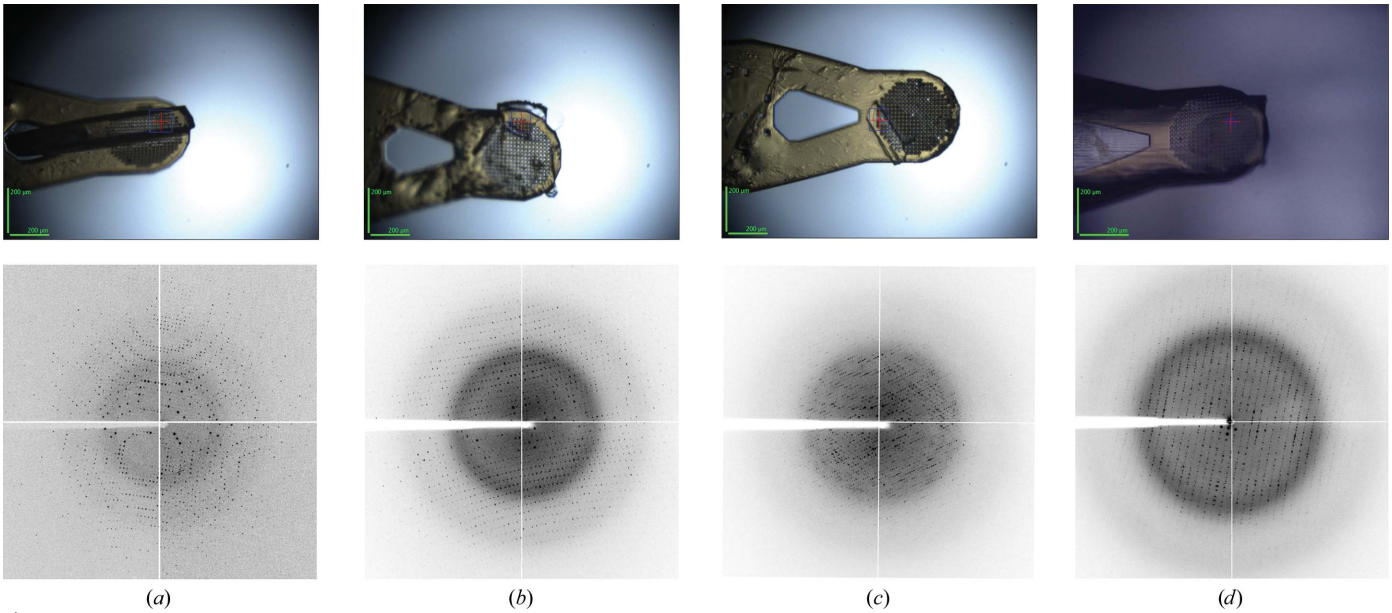

Figure 1
Images of protein crystals and corresponding diffraction images after cryocooling in the absence of liquid. (*a*) Trypsin; the inscribed circle of the detector (ICD) is set to 1.4 Å. (*b*) *β*PGM, ICD 1.7 Å. (*c*) RhoA, ICD 1.8 Å. (*d*) hPGK, ICD 2.0 Å. The red cross indicates the centre of the X-ray beam and the blue square shows the beam size.

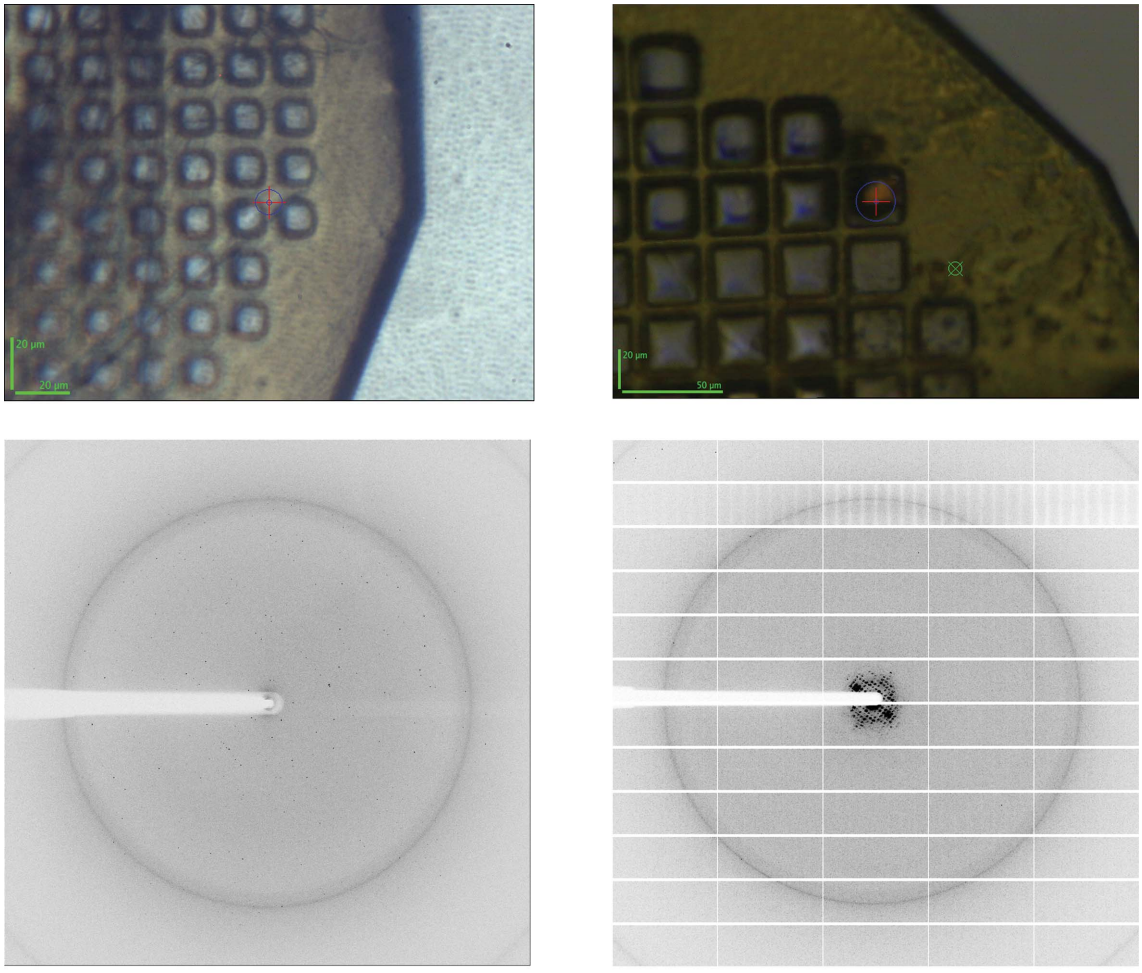

(*a*) (*b*)

Figure 2
Images of protein microcrystals and corresponding diffraction images after cryocooling in the absence of liquid. (*a*) hPGK with bound L-ADP, ICD 2.9 Å; (*b*) a microcrystal of the outer membrane protein DR2577 from *D. radiodurans*, ICD 3.0 Å. Weak ice rings are observed in both images as some mother liquor remains in the mesh. The red cross indicates the centre of the X-ray beam and the blue circle shows the beam size.

reduced to 50 × 33 Å and are further reduced to 40 × 31 Å in the final state. This places an upper limit on the largest dimension of the solvent channels within crystals that can prevent the formation of ice crystals at 40 Å. This value will presumably be subject to some variation owing to the exact configuration of the symmetry-related molecules and the composition of the mother liquor. This method of cryocooling may therefore be ineffective for crystals of macromolecules containing solvent channels larger than 40 Å in diameter. As crystals with solvent channels of these dimensions tend to be unusual, the technique should be applicable to most systems.

We have shown for a number of different systems that it is possible to cryocool crystals by removing the surrounding mother liquor. This potentially removes a major bottleneck in protein structure solution and has other benefits such as reduced X-ray background scattering and absorption (crucial when trying to measure small anomalous differences) and easier visualization of samples. It also removes the need to exactly match the composition of the mother liquor in the cryoprotection solution; this is particularly problematic with membrane proteins. In cases where ligands are being screened, such as high-throughput fragment-based drug discovery (Murray & Blundell, 2010), it also removes the need to use additional material and match original concentrations. This protocol does have disadvantages compared with traditional loop mounting. Mesh loops will not be suitable for all samples as they can bend delicate crystals that are better supported in an amorphous glass, and while visualizing the sample is simple on the obverse of the loop it can be difficult from the reverse, although this depends on the crystal size and shape. While the automation of synchrotron beamlines has enabled a large increase in the number of crystals studied (Bowler *et al.*, 2010; Beteva *et al.*, 2006; Okazaki *et al.*, 2008; Snell *et al.*, 2004; Zhang *et al.*, 2006), sample harvesting remains a manual process that could benefit from automation (Berger *et al.*, 2010; Kitago *et al.*, 2010; Viola *et al.*, 2007). The removal of cryoprotectant screening would eliminate a major hurdle in this procedure and facilitate automation. While this study is not exhaustive, it has been shown that the technique is applicable to both large and small crystals of different types with solvent channels typical of most crystals of macromolecules. We hope that this will stimulate others to attempt this method of cryoprotection and to use this protocol in the development of automated crystal-harvesting systems.

We thank Stephen Gamblin (NIMR, London, England) for the gift of the plasmid bearing human RhoA, Jon Waltho, Jin Yi and the members of the Biological NMR group (Department of Molecular Biology and Biotechnology, University of Sheffield, England) for

assistance in the expression and purification of RhoA and β-PGM, and Ulrike Kapp for excellent technical assistance. The authors are grateful to Gordon Leonard (ESRF, Grenoble) for helpful discussions and careful reading of the manuscript and the two reviewers for providing valuable comments and suggestions.

References

Alcorn, T. & Juers, D. H. (2010). *Acta Cryst.* D**66**, 366–373.
Baxter, N. J., Bowler, M. W., Alizadeh, T., Cliff, M. J., Hounslow, A. M., Wu, B., Berkowitz, D. B., Williams, N. H., Blackburn, G. M. & Waltho, J. P. (2010). *Proc. Natl Acad. Sci. USA*, **107**, 4555–4560.
Berejnov, V., Husseini, N. S., Alsaied, O. A. & Thorne, R. E. (2006). *J. Appl. Cryst.* **39**, 244–251.
Berger, M. A., Decker, J. H. & Mathews, I. I. (2010). *J. Appl. Cryst.* **43**, 1513–1518.
Beteva, A. *et al.* (2006). *Acta Cryst.* D**62**, 1162–1169.
Bourenkov, G. P. & Popov, A. N. (2010). *Acta Cryst.* D**66**, 409–419.
Bowler, M. W., Guijarro, M., Petitdemange, S., Baker, I., Svensson, O., Burghammer, M., Mueller-Dieckmann, C., Gordon, E. J., Flot, D., McSweeney, S. M. & Leonard, G. A. (2010). *Acta Cryst.* D**66**, 855–864.
Bowler, M. W., Montgomery, M. G., Leslie, A. G. W. & Walker, J. E. (2006). *Acta Cryst.* D**62**, 991–995.
Chen, X., Weber, I. & Harrison, R. W. (2008). *J. Phys. Chem. B*, **112**, 12073–12080.
Chinte, U., Shah, B., DeWitt, K., Kirschbaum, K., Pinkerton, A. A. & Schall, C. (2005). *J. Appl. Cryst.* **38**, 412–419.
Cliff, M. J., Bowler, M. W., Varga, A., Marston, J. P., Szabó, J., Hounslow, A. M., Baxter, N. J., Blackburn, G. M., Vas, M. & Waltho, J. P. (2010). *J. Am. Chem. Soc.* **132**, 6507–6516.
Flot, D., Mairs, T., Giraud, T., Guijarro, M., Lesourd, M., Rey, V., van Brussel, D., Morawe, C., Borel, C., Hignette, O., Chavanne, J., Nurizzo, D., McSweeney, S. & Mitchell, E. (2010). *J. Synchrotron Rad.* **17**, 107–118.
Gabadinho, J. *et al.* (2010). *J. Synchrotron Rad.* **17**, 700–707.
Garman, E. (1999). *Acta Cryst.* D**55**, 1641–1653.
Garman, E. F. & Mitchell, E. P. (1996). *J. Appl. Cryst.* **29**, 584–587.
Garman, E. F. & Schneider, T. R. (1997). *J. Appl. Cryst.* **30**, 211–237.
Hope, H. (1988). *Acta Cryst.* B**44**, 22–26.
Incardona, M.-F., Bourenkov, G. P., Levik, K., Pieritz, R. A., Popov, A. N. & Svensson, O. (2009). *J. Synchrotron Rad.* **16**, 872–879.
Jiang, J.-S. & Brünger, A. T. (1994). *J. Mol. Biol.* **243**, 100–115.
Juers, D. H. & Matthews, B. W. (2004*a*). *Acta Cryst.* D**60**, 412–421.
Juers, D. H. & Matthews, B. W. (2004*b*). *Q. Rev. Biophys.* **37**, 105–119.
Kiefersauer, R., Than, M. E., Dobbek, H., Gremer, L., Melero, M., Strobl, S., Dias, J. M., Soulimane, T. & Huber, R. (2000). *J. Appl. Cryst.* **33**, 1223–1230.
Kitago, Y., Watanabe, N. & Tanaka, I. (2005). *Acta Cryst.* D**61**, 1013–1021.
Kitago, Y., Watanabe, N. & Tanaka, I. (2010). *J. Appl. Cryst.* **43**, 341–346.
Kwong, P. D. & Liu, Y. (1999). *J. Appl. Cryst.* **32**, 102–105.
Lallemand, P., Chaloin, L., Roy, B., Barman, T., Bowler, M. W. & Lionne, C. (2011). *J. Mol. Biol.* **409**, 742–757.
Murray, C. W. & Blundell, T. L. (2010). *Curr. Opin. Struct. Biol.* **20**, 497–507.
Okazaki, N., Hasegawa, K., Ueno, G., Murakami, H., Kumasaka, T. & Yamamoto, M. (2008). *J. Synchrotron Rad.* **15**, 288–291.
Parkin, S. & Hope, H. (1998). *J. Appl. Cryst.* **31**, 945–953.
Pflugrath, J. W. (2004). *Methods*, **34**, 415–423.
Rodgers, D. W. (1994). *Structure*, **2**, 1135–1140.
Russi, S., Juers, D. H., Sanchez-Weatherby, J., Pellegrini, E., Mossou, E., Forsyth, V. T., Huet, J., Gobbo, A., Felisaz, F., Moya, R., McSweeney, S. M., Cusack, S., Cipriani, F. & Bowler, M. W. (2011). *J. Struct. Biol.* **175**, 236–243.
Sanchez-Weatherby, J., Bowler, M. W., Huet, J., Gobbo, A., Felisaz, F., Lavault, B., Moya, R., Kadlec, J., Ravelli, R. B. G. & Cipriani, F. (2009). *Acta Cryst.* D**65**, 1237–1246.
Snell, G., Cork, C., Nordmeyer, R., Cornell, E., Meigs, G., Yegian, D., Jaklevic, J., Jin, J., Stevens, R. C. & Earnest, T. (2004). *Structure*, **12**, 537–545.
Teng, T.-Y. (1990). *J. Appl. Cryst.* **23**, 387–391.
Teng, T.-Y. & Moffat, K. (1998). *J. Appl. Cryst.* **31**, 252–257.
Thorne, R. E., Stum, Z., Kmetko, J., O'Neill, K. & Gillilan, R. (2003). *J. Appl. Cryst.* **36**, 1455–1460.
Viola, R., Carman, P., Walsh, J., Miller, E., Benning, M., Frankel, D., McPherson, A., Cudney, B. & Rupp, B. (2007). *J. Appl. Cryst.* **40**, 539–545.
Warkentin, M., Berejnov, V., Husseini, N. S. & Thorne, R. E. (2006). *J. Appl. Cryst.* **39**, 805–811.
Warkentin, M. & Thorne, R. E. (2009). *J. Appl. Cryst.* **42**, 944–952.
Weik, M. & Colletier, J.-P. (2010). *Acta Cryst.* D**66**, 437–446.
Weik, M., Kryger, G., Schreurs, A. M. M., Bouma, B., Silman, I., Sussman, J. L., Gros, P. & Kroon, J. (2001). *Acta Cryst.* D**57**, 566–573.
Zerrad, L., Merli, A., Schröder, G. F., Varga, A., Gráczer, É., Pernot, P., Round, A., Vas, M. & Bowler, M. W. (2011). *J. Biol. Chem.* **286**, 14040–14048.
Zhang, Z., Sauter, N. K., van den Bedem, H., Snell, G. & Deacon, A. M. (2006). *J. Appl. Cryst.* **39**, 112–119.